Transactions of the Materials Research Society of Japan 31[1] 23-26 (2006)

Electronic Structure in the Valence Band of (Pb,La)(Zr,Ti)O_3 Thin Films Probed by Soft-X-Ray Emission Spectroscopy

Tohru Higuchi,[1] Takeyo Tsukamoto,[1] Takeshi Hattori,[1] Yoshihisa Honda,[2]
Shintaro Yokoyama[2] and Hiroshi Funakubo[2]
[1] Department of Applied Physics, Tokyo University of Science, 1-3 Kagurazaka, Shinjuku, Tokyo 162-8601, Japan
[2] Department of Innovative and Engineered Materials, Tokyo Institute of Technology, Yokohama 226-8502, Japan
Fax: +81-3-5228-8241, e-mail: higuchi@rs.kagu.tus.ac.jp

The electronic structure of (Pb,La)(Zr,Ti)O_3 thin film has been studied by soft-X-ray spectroscopy. The valence band is in good accordance with the band calculation. The valence band is mainly composed of the O 2*p* states hybridized with Ti 3*d* and Pb 6*s* states. The hybridization effect between the Ti 3*d* and O 2*p* states increases with La substitution, indicating the change of Ti-O bond length the *a*-*b* plane. The hybridization effect between the Pb 6*s* and O 2*p* states decreases with La substitution. The Pb-O hybridization effect is considered to be closely related to the ferroelectric and optical behaviors.

Key words: (Pb,La)(Zr,Ti)O_3, thin film, soft-X-ray spectroscopy, electronic structure, hybridization effect

1. INTRODUCTION

Ferroelectric (Pb,La)(Zr,Ti)O_3 has been widely investigated for nonvolatile ferroelectric random access memories application [1] as well as microelectromechanical system [2] sensors and actuators because of their superior characteristics with large remanent polarization and piezoelectric coefficients. PZT films are required to be deposited on silicon substrates due to the good compatibility with silicon technologies. Therefore, PZT high quality films have been prepared by several deposition techniques, such as metalorganic vapor deposition (MOCVD) [3-9], sol-gel [10-13] and sputtering methods [14]. The structural and electrical properties have been also extensively studied in the PZT films. On the other hand, we believe that understanding the electronic structure of PZT thin film is also one of the most important considerations for its further applications. On the other hand, understanding the electronic structure of (Pb,La)(Zr,Ti)O_3 thin film is also important subject for further application.

In this study, the electronic structure in the valence band region of (Pb,La)(Zr,Ti)O_3 thin films has been probed by soft-X-ray emission spectroscopy (SXES). SXES can confirm the electronic structure in the bulk state, because the mean free path of a soft-X-ray is very long compared with that of an electron. The SXES spectra, which have clear selection rules regarding the angular momentum due to dipole transition, reflect the occupied partial density-of-state (DOS) [15-20]. As reference, the Ti 2*p* X-ray absorption spectroscopy (XAS) spectra were also measured in order to obtain the magnitude of crystal-field splitting, which is closely related with the lattice constant. The XAS is related directly to the unoccupied DOS. This optical process is rather local process, because of the localized core state. It is governed by dipole selection rules so that XAS gives the spectrum related to the site- and symmetry-selected DOS [21-24].

2. EXPERIMENTAL

(Pb,La)(Zr,Ti)O_3 thin films were prepared on (100) MgO substrates at 600°C by MOCVD. $Pb(C_{11}H_{19}O_2)_2$, $La(C_{13}H_{25}O_2)_3$, $Zr(O{\cdot}t\text{-}C_4H_9)_4$, and $Ti(O{\cdot}t\text{-}C_3H_7)_4$ were used as Pb, La, Zr, and Ti source materials, respectively [3-7]. Oxygen was used as an oxidant. The source gas flow was led to the substrate through a nozzle in a cold-wall vertical reaction chamber. The compositions of the (Pb,La)(Zr,Ti)O_3 thin films are shown in Table 1. The film thickness is fixed at 700 nm. The crystal structure and orientation of the films were characterized with an X-ray diffractometer (PANalytical X'Pert-MRD). These thin films exhibited (001) and (002) orientations.

Table 1: Compositions of La, Zr and Ti of (Pb,La)(Zr,Ti)O_3 thin films

Sample	La	Zr	Ti	(Pb+La)/(Pb+La+Zr+Ti)
PZT	0	33	67	51
PLZT-3	3	32	68	52
PLZT-6	6	36	64	51

XAS and SXES measurements were carried out at the revolver undulator beamline BL-19B at the Photon Factory of the High Energy Accelerator Organization, in Tsukuba, Japan. High brightness and high resolution were realized using a varied- line-spacing plane grating monochrometer. The XAS spectra were measured by a Si photodiode. The SXES spectra were measured by a soft-X-ray emission spectrometer. The spectrometer used the Rowland circle geometry that consisted of a grating with a groove density of 300 lines/mm and a Cs-coated multichannel detector. The total resolutions of XAS and SXES were approximately 0.1 eV and 0.4 eV, respectively, at *hν*=450 eV.

3. RESULTS AND DISCUSSION

Figure 1 shows Ti 2*p* XAS spectra as a function of La concentration in (Pb,La)(Zr,Ti)O$_3$ thin films. The details of samples (PZT, PLZT-3, PLZT-6) are shown in Table 1. The Ti 2*p* XAS spectra correspond to the transition from the Ti 2*p* core level to the unoccupied Ti 3*d* state. The spectra are derived from the two parts of L$_3$ (2$p_{3/2}$) and L$_2$ (2$p_{1/2}$). They are split into the t_{2g}- and e_g-subbands by the octahedral ligand field [20,24]. Comparing each spectra, the intensities of the four peaks do not depend strongly on La substitution. This result indicates that the La ions do not enter the Ti^{4+} site. The energy separation between t_{2g}- and e_g-subbands corresponds to the crystal-field splitting (10Dq). The 10Dq increases from 2.2 eV to 2.4 eV. According to the ligand-field theory, the magnitude of 10Dq is determined by ion radius, electron mass, element number, and lattice constant. The lattice constant is in inverse proportion to 10Dq. The 10Dq increases with increasing La concentration. This result agrees with the decreases of lattice constant in (Pb,La)(Zr,Ti)O$_3$.

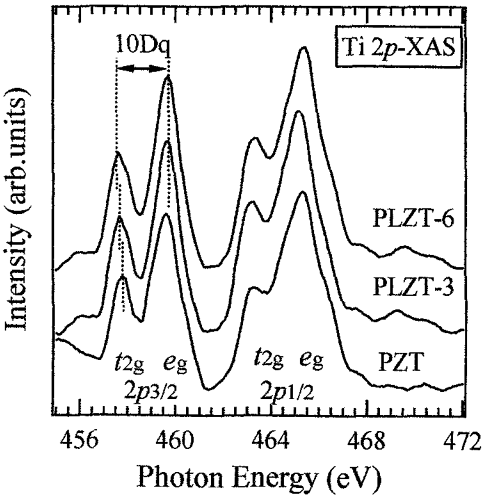

Fig. 1: Ti 2*p* XAS spectra as a function of La concentration in (Pb,La)(Zr,Ti)O$_3$ thin films. The energy separation between the t_{2g}- and e_g-subbands reflects the magnitude of crystal-field splitting (10Dq).

Figure 2 shows the SXES spectra of PLZT-6 thin film. The SXES spectra reflect the band structure of the valence band. The valence band consists of three structures denoted by peaks A, B and C. As a reference, the calculated total-DOS and partial-DOS (PDOS) are shown under each SXES spectra. The electronic structure calculations based on the density functional theory using the local density approximation (LDA) were performed using an *ab-initio* calculation program [25]. To calculate the electronic structure, we optimized the basis sets with the effective core potential. In this calculation, the composition of PZT is PbZr$_{0.65}$Ti$_{0.35}$O$_3$. The lattice constants along the *a*- and *c*-axes are 3.97 Å and 4.14 Å, respectively. The calculated total-DOS curves are obtained by convoluting the original PDOS with Gaussian broadening functions with a width of 0.5 eV, which corresponds to the total resolution of the experimental system. The line shape, bandwidth and peak positions of total-DOS are in good accordance with those of the SXES spectra. From these agreements, we can assign the detailed structures of the valence band and conduction band. The A peak consists of the Pb 6*s* state hybridized with the O 2*p* state. A contribution from Pb 6*p* is not found in the valence band region. The B and C peaks consist of the Ti 3*d* state hybridized with the O 2*p* state. The Ti 3*d* contribution is more significant in the higher energy region in which the O 2*p* state has a larger admixture of the Ti 3*d* state. Thus, peak B corresponds to the nonbonding state and peak C corresponds to the bonding state that is well mixed with the Ti 3*d* state.

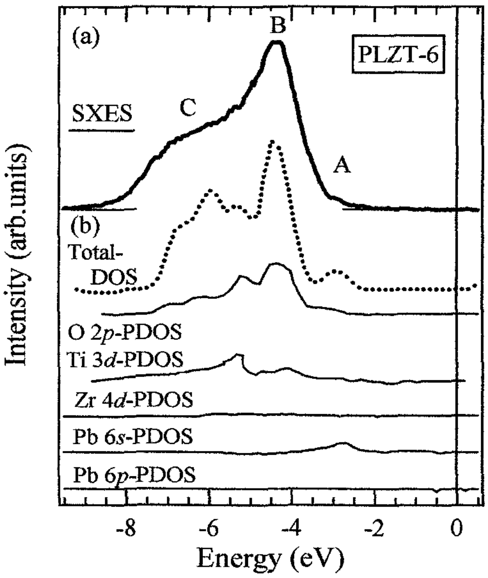

Fig. 2 (a) Total-DOS of PLZT-6 thin film. The SXES spectra reflect the valence band. (b) Calculated band total-DOS (dashed line) and PDOS (solid line) are shown under each spectrum.

Figure 3 shows the O 1*s* and Ti 2*p* SXES spectra of PZT, PLZT-3 and PLZT-6 thin films. The intensities of the SXES spectra are normalized by the intensity of the elastic scattering, although the elastic peak scattering peak is not shown in this figure. The clear selection rule of SXES exhibits mainly within the same atomic species, because the core hole is strongly localized. For this reason, the O 1*s* and Ti 2*p* SXES spectra reflect the O 2*p* PDOS and Ti 3*d* PDOS, respectively. The obtained O 2*p* PDOS and Ti 3*d* PDOS correspond to the band structure in the valence band region. It is striking that the energy position of the O 2*p* PDOS overlaps with that of the Ti 3*d* PDOS. This result indicates that the O 2p state hybridizes with the Ti 3*d* state in the valence band, as shown in the band calculation in Fig. 2. Comparing the spectra, the bandwidths of the O 2*p* and Ti 3*d* states in PLZT-6 thin film are in good agreement with those in PZT and PLZT-3 thin films. It is notable that the intensity of Ti 3*d* PDOS increases with La concentration. This finding indicates that the hybridization effect between the Ti 3*d* and O 2*p* states increases with increasing La concentration. The

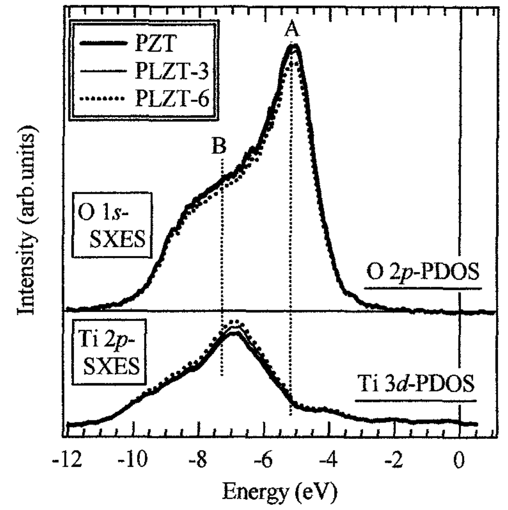

Fig. 3 O 1*s* and Ti 2*p* SXES spectra as a function of La concentration in $(Pb,La)(Zr,Ti)O_3$ thin films. The O 1*s* and Ti 2*p* SXES spectra reflect the O 2*p* PDOS and Ti 3*d* PDOS, respectively.

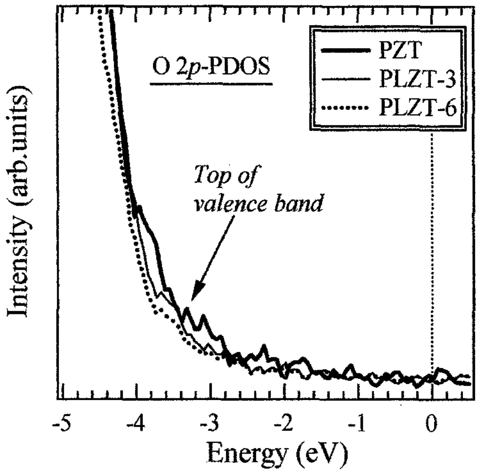

Fig. 4 O 2p PDOS at the top of the valence band as a function of La concentration in $(Pb,La)(Zr,Ti)O_3$ thin films. Arrow indicates the top of the valence band. The PDOS reflect the O *2p* PDOS hybridized with Pb 6s PDOS.

difference of the Ti-O hybridization effect contributes to the change in Ti-O bond length with the decrease in lattice constant.

Figure 4 shows the detailed O 1*s* SXES spectra at the top region of the valence band as a function of La concentration in $(Pb,La)(Zr,Ti)O_3$ thin films. The top of the valence band denoted by peak A corresponds to the Pb 6*s* state hybridized with the O 2*p* state, as shown in the band calculation in Fig. 2. Comparing the detailed O 1*s* SXES spectra, the intensity of peak A is smaller in PLZT thin film. This finding indicates that the hybridization effect between the Pb 6*s* and O 2*p* states is lower in PLZT thin film. The decrease of the Pb-O hybridization effect in PLZT thin film contributes to La substitution at the Pb site. On one hand, this result may indicate that the Pb-O hybridization effect plays an important role in the ferroelectric and piezoelectric properties of PZT. The Pb 6*s* orbital is fully occupied and acts as a lone pair state. A similar fact has been reported in the band calculation by Cohen and Krakauer [26-28]. The Pb 6*s* state is asymmetric and the Pb lone pair lies off center in the PbO plane. The ferroelectric behavior is amplified by the off-center displacement of Pb in PZT. The displacement is considered to be driven by the lone pair *s* electrons, although its origin has not been clarified in detail in this study.

4. CONCLUSION

We have studied the electronic structures of $(Pb,La)(Zr,Ti)O_3$ thin films using XAS and SXES. The valence band and conduction band determined by XAS and SXES spectra are in good accordance with the band calculation. The valence bands of PZT and PLZT thin films are mainly composed of the O 2*p* state hybridized with Ti 3*d* and Pb 6*s* states. The hybridization effect between the Ti 3*d* and O 2*p* states is larger in PLZT thin film, indicating the change in Ti-O bond length with the decrease of lattice constant. The hybridization effect between the Pb 6*s* and O 2*p* states is smaller in PLZT thin film. The Pb-O hybridization effect is considered to be closely related with the ferroelectric behavior.

ACKNOWLEDGEMENT

We would like to thank Prof. Shik Shin for his valuable discussion. This work was partly supported by the Grant-In-Aid for Science Research from the Ministry of Education, Culture, Sports, Science and Technology of Japan.

REFERENCES

[1] J. Scott and C. Paz de Araujo: Science **246** (1989) 1400.
[2] N. Setter: Piezoelectric Materials in Devices, ed. N. Setter (EPFL Swiss Federal Institute of Technology, Switzerland, 2002) 1.
[3] K. Nagashima and H. Funakubo: Jpn. J. Appl. Phys. **39** (2000) 212.
[4] S. Yokoyama, Y. Honda, H. Morioka, G. Asano, T. Oikawa, T. Iijima, H. Matsuda and H. Funakubo: Jpn. J. Appl. Phys. **42** (2003) 5922.
[5] S. Okamoto, S. Yokoyama, Y. Honda, G. Asano and H. Funakubo: Jpn. J. Appl. Phys. **43** (2004) 6567.
[6] G. Asano, T. Oikawa and H. Funakubo: Jpn. J. App. Phys. **42** (2003) 2801.
[7] Y. Honda, S. Yokoyama and H. Funakubo: Trans. Mater. Res. Soc. Jpn. **28** (2003) 157.
[8] M. Miyake, K. Lee, S. Kawasaki, Y. Ueda, S. Okamura and T. Shiosaki: Jpn. J. Appl. Phys. **41** (2002) 241.
[9] M. Shimizu, M. Okaniwa, H. Fujisawa and H. Niu: Jpn. J. Appl. Phys. **41** (2002) 6686.
[10] S. Okamura, R. Takeuchi and T. Shiosaki: Jpn. J. Appl. Phys. **41** (2002) 6714.
[11] Z. Wei, K. Yamashita and M. Okuyama: Jpn. J.

Appl. Phys. **40** (2001) 5539.

[12] H. Xu, T. Kiyomoto, Y. Morikawa, M. Okuyama and C. Lin: Jpn. J. Appl. Phys. **37** (1998) L809.

[13] T. Kijima and H. Ishiwara: Jpn. J. Appl. Phys. **41** (2002) L716.

[14] M. Kurita, S. Okamura and T Shiosaki: Jpn. J. Appl. Phys. **43** (2004) 4124.

[15] T. Higuchi, T. Tsukamoto, M. Watanabe, M. M. Grush, T. A. Callcott, R. C. Perera, D. L. Ederer, Y. Tokura, Y. Harada, Y. Tezuka and S. Shin: Phys. Rev. B **60** (1999) 7711.

[16] T. Higuchi, K. Kudoh, T. Takeuchi, Y. Masuda, Y. Harada, S. Shin and T. Tsukamoto: Jpn. J. Appl. Phys. **41** (2002) 7195.

[17] T. Higuchi, T. Tsukamoto, K. Oka, T. Yokoya, Y. Tezuka and S. Shin: Jpn. J. Appl. Phys. **38** (1999) 5667.

[18] T. Higuchi, T. Tsukamoto, N. Sata, M. Ishigame, Y. Tezuka and S. Shin: Phys. Rev. B **57** (1998) 6978.

[19] T. Higuchi, Y. Moriuchi, Y. Noguchi, M. Miyayama, S. Shin and T. Tsukamoto: Jpn. J. Appl. Phys. **42** (2003) 6226.

[20] T. Higuchi, T. Tsukamoto, T. Hattori, Y. Honda, S. Yokoyama and H. Funakubo: Jpn. J. Appl. Phys. **44** (2005) 6923.

[21] J. C. Fuggle and J. E. Inglesfield: Unoccupied Electronic States (Springer-Verlag, city, 1991).

[22] T. Higuchi, T. Tsukamoto, K. Kobayashi, Y. Ishiwata, M. Fujisawa, T. Yokoya, S. Yamaguchi and S. Shin: Phys. Rev. B **61** (2000) 12860.

[23] T. Higuchi, T. Tsukamoto, K. Kobayashi, S. Yamaguchi, Y. Ishiwata, N. Sata, K. Hiramoto, M. Ishigame and S. Shin: Phys. Rev. B **65** (2002) 33201.

[24] A. Kotani and S. Shin: Rev. Mod. Phys. **73** (2001) 203.

[25] J. Robertson, W. L. Warren and B. A. Tuttle: J. Appl. Phys. **77** (1995) 3975.

[26] R. E. Cohen: Nature **358** (1992) 136.

[27] R. E. Cohen and H. Krakauer: Phys. Rev. B **42** (1990) 6416.

[28] S. -H. Wei and H. Krakauer: Phys. Rev. Lett. **55** (1985) 1200.

(Received December 10, 2005; Accepted January 31, 2006)